Research Article

Infrared Spectrum Analysis of Goji Berry during Electrohydrodynamic Drying

Jiabao Ni,[1] Changjiang Ding (ID),[1] Yaming Zhang,[1] Zhiyuan Cao,[1] Zhiqing Song,[1] Xiuzhen Hu (ID),[1] and Tingjie Hao[2]

[1]*College of Science, Inner Mongolia University of Technology, Hohhot, China*
[2]*Institute of Metrology and Testing of Inner Mongolia, Hohhot, China*

Correspondence should be addressed to Changjiang Ding; ding9713@163.com

This paper aims to study the effects of different needle spacings on goji berry structure during electrohydrodynamic (EHD) drying. The drying characteristics and the product quality parameters of goji berry during the drying process were measured. The infrared spectrum of the dried product was analyzed in detail. The results showed that the average drying rate of goji berry under different needle spacing conditions was significantly higher than that of the control group, and the average drying rate decreased with the increase of needle spacing. The change of needle spacing has great influence on goji berry polysaccharide content and flavonoid content. Fourier transform infrared spectroscopy showed that the infrared spectra of goji berry in each treatment group were generally similar. The first-order infrared spectra of different treatment groups were mainly different in the range of 1740 cm^{-1} and 2800 cm^{-1}–2950 cm^{-1}. The shape and intensity of the absorption peaks of the second derivative infrared spectrum of goji berry in different needle spacing treatment groups were different. When the needle spacing is 2 cm and 4 cm, there is a highly variant peak ratio and a low common peak ratio, which proves that the best drying effect is at 2 cm and 4 cm. It provides experimental and theoretical basis for the study of the application and drying mechanism of infrared spectroscopy in the field of electrohydrodynamic drying.

1. Introduction

Goji berry contains polysaccharides, flavonoids, carotenoids, vitamin C, scutellarin, amino acids, and trace elements and other nutrients and has very high medicinal value, such as strengthening the immune system, lowering blood sugar, lowering blood fat, and fighting tumors [1–5]. However, the storage period of fresh goji fruits is very short. It is easy to mold and rot and must be dried to store for a long time. At present, drying technology of goji berries mainly includes natural drying, hot-air drying [6], vacuum drying [7], and microwave drying [8]. However, the above drying technology has its own disadvantages; that is, the products of natural drying and hot-air drying are poor, vacuum drying equipment is extremely expensive, the products of microwave drying are not uniform. Therefore, it is very necessary to study new goji berry drying technology.

In recent years, researchers have explored a new type of nonthermal drying technology—electrohydrodynamic drying technology—and achieved good results [9–12]. The electrohydrodynamic drying technology has many advantages, such as fast drying speed, no damage to effective nutrients, sterilization, energy conservation and no pollution to the environment, etc. Yu et al. studied the electrohydrodynamic drying technology to dry potatoes and found that electrohydrodynamic drying not only accelerated the drying speed of potatoes, but also effectively protected the effective components [13]. Ding et al. used an electrohydrodynamic drying device to dry carrot slices and found that carotene was 1.1153 times higher than the control [14]. Esehaghbeygi et al. took bananas as the experimental material and carried out the drying experiment in the electrohydrodynamic drying equipment; the results showed that, compared with microwave drying, the bananas under

electrohydrodynamic drying had better rehydration ability, appearance, and quality [15]. Bai et al. dried the sea cucumber using electrohydrodynamic drying and found that the energy consumption under electrohydrodynamic drying is only 21.31% of the hot-air drying and the protein content is higher than that of the hot-air drying [16]. Previously, we used the electrohydrodynamic drying to dry the goji berry and achieved very satisfactory results [17, 18].

Infrared spectroscopy technology has recently been favored by researchers because of its nondestructive, nonchemical reagents, simple operation, low sample consumption, and good repeatability and has become an important analytical method [19]. Zhuang et al. used infrared spectroscopy to effectively identify yam samples from four different regions and accurately analyzed total sugar, polysaccharides, and flavonoids in yam samples [20]. Acril et al. successfully classified foods by analyzing the differences in infrared absorption peaks of different varieties of garlic in different regions [21]. Tingting et al. combined infrared spectroscopy and chemical testing to analyze goji berry samples from four different producing areas and successfully established a predictive flavonoid model [22]. Arslan et al. successfully quantitatively analyzed the chemical composition of black goji berry samples by means of infrared spectroscopy and chemometrics [23]. Although these studies are detailed and elaborated, there is no detailed report about the analysis of goji berry dried electrohydrodynamically by infrared spectrum. So, it is necessary to conduct in-depth research.

In this work, the drying characteristics and quality of goji berries were studied under different needle spacing conditions in an electrohydrodynamic system. We measured the drying characteristics of goji berry such as average drying rate and average drying time, as well as quality parameters such as polysaccharide content and flavonoid content. The effects of electrohydrodynamic drying on microstructure of goji berry were studied by means of first-order infrared spectroscopy, second-order infrared spectroscopy, infrared spectral peak intensity ratio, two-index sequence analysis of common peak ratio, and variant peak ratio of infrared fingerprints. It provides an experimental and theoretical basis for further exploration of the drying mechanism of goji berry in an electrohydrodynamic system.

2. Materials and Methods

2.1. Experimental Device. The experimental device is shown in Figure 1. It consists mainly of high-voltage power supply (YD (JZ)-1.5/50, Wuhan, China), controller (KZX-1.5KVA, Wuhan, China), and multineedle-to-plate electrode system. The high-voltage power supply outputs AC voltage, and the adjustment range of the controller is from 0 kV to 50 kV. The multineedle electrode is connected to the high-voltage power supply. The needle spacing between adjacent needles can be adjusted, and the adjustment range is from 2 cm to 12 cm. Each needle has a length of 60 mm and a diameter of 1 mm. The ground electrode is a $100 \, cm \times 45 \, cm$ stainless steel plate. A microampere meter is connected between the steel plate and the ground to measure the current generated
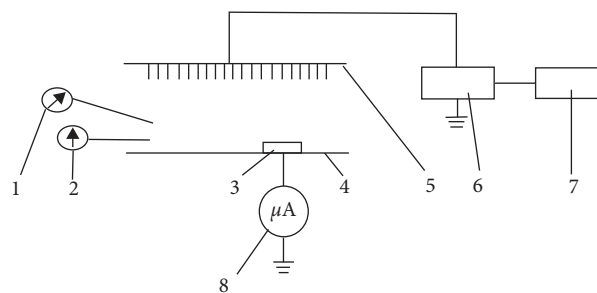

Figure 1: Schematic diagram of electrohydrodynamic (EHD) drying. (1) Hygrometer. (2) Thermometer. (3) Sample. (4) Ground electrode. (5) Needle electrode. (6) High-voltage power supply. (7) Control system. (8) Microammeter.

during the experiment. The current varies with the needle spacing and ranges from $0.06 \, \mu A$ to $0.12 \, \mu A$ during the drying experiment. The distance between the needlepoint and the steel plate is 10 cm.

2.2. Determination of Initial Moisture Content. Fresh goji berry were purchased from local growers in Tuoketuo County, Hohhot, Inner Mongolia, and immediately placed in a 4°C refrigerator for experimental needs. The initial moisture content of fresh goji berries was measured using a moisture rapid tester (Sh10 A, Shanghai). After three independent measurements, the average value was taken. The results showed that the fresh fruits had a moisture content of $78 \pm 1\%$.

2.3. Experimental Method. All drying experiments of goji berries were conducted at a constant temperature of $25°C \pm 2°C$, a relative humidity of $30\% \pm 2\%$, and a laboratory environment wind speed of 0 m/s. The wet air is continuously blown into the environment electrohydrodynamically (EHD). Due to a few materials in the drying process, the influence of wet air on the environment is very small. So, the exchange of wet air can be neglected in drying experiment. All electrohydrodynamic drying experiments of goji berries were conducted at an electrode distance of 10 cm, a corresponding voltage of 30 kV, and a multineedle-to-plate electrode system. The range of needle spacing is from 2 cm to 12 cm and the needle spacing was changed every 2 cm. At the same time, goji berry dried in the laboratory environment was used as the control group at 0 kV.

During electrohydrodynamic drying experiment, the Sartorius electronic balance (BS124S, Germany) was used to record the mass of goji fruits every one hour, and then the average drying time and drying rate of the goji were calculated according to the formula. Each experiment was repeated 3 times independently, and the results were expressed as mean ± standard deviation (SD).

2.4. Determination of Average Drying Time and Average Drying Rate. The time required to reduce the moisture content of goji berries from 78% to 10% was determined as the average drying time. The average drying rate represents

the evaporation of water per unit time and per unit area in the material. The average drying rate of goji berries is calculated using the following equation [24]:

$$DR = \frac{m_o - m_i}{S\Delta t},$$

(1)

where DR is the average drying rate, m_o is the initial mass of goji berry fruit, m_i is the mass of the goji fruit dried to a moisture content of 10%, Δt is the average drying time, and S is the cross-sectional area of the goji berries during drying process.

2.5. Determination of Flavonoid Content.

The total flavonoid content of the extracts was determined using a colorimetric method described by Zhao et al. [6]. We placed the extraction solution and $NaNO_2$ solution in a 10 mL centrifuge tube. After 6 min, aluminium nitrate solution (0.4 mL, 100 g/kg) was added to the mixture and allowed to stand for 6 min, before NaOH solution (4 mL, 40 g/kg) was added. After 15 min, methanol aqueous solution was added immediately to a volume of 10 mL. The absorbance against the blank was determined at 510 nm by spectrophotometry. The total flavonoid content was expressed as mg of rutin equivalents (RE) per g of dry weight at concentrations of 0.1 mg/mL–1.0 mg/mL.

2.6. Determination of Polysaccharide Content.

The polysaccharide content was determined by the colorimetric method described by Xie et al. [25]. To remove the pigments in wolfberry, 2 g of dried wolfberry samples was powdered and mixed with 100 mL absolute ether before the Soxhlet extraction at 45°C for 2 h. The pigments were extracted with 80 mL distilled water in bath at 50°C and constant vibration at 120 r/min for 3 h and the residues were removed. Then supernatants were concentrated under reduced pressure at temperature not exceeding 40°C and precipitated with 80 mL 95% cooled ethanol (4 v/v). After 48 h under refrigeration (4°C) storage, the sample was centrifuged at 5.000 g for 15 min at 4°C. The precipitated polysaccharides were filtered and washed twice with absolute ethanol to obtain the crude water-soluble polysaccharides. The extracting solution of crude water-soluble polysaccharides was diluted at a volume ratio of 5 : 1 (distilled H_2O: crude polysaccharides). One milliliter of the diluted solution, 1 mL of phenol at 5 g/100 mL, and 5 mL of concentrated sulfuric acid were added to the tubes. It was allowed to settle for 15 min in bath at 40°C. The sample's absorbance was determined at 490 nm using UV-VIS spectrophotometer. The total polysaccharides content was estimated by comparison with a standard curve.

2.7. Determination of Infrared Spectrum.

After sieving, the dried goji berry fruit product was pulverized with agate mortar and mixed with potassium bromide. It was placed in a tableting machine (HY-12, China) to form a tablet. The sample was scanned with a Fourier transform infrared spectrometer (Nicolet iS10, USA), and the interference of water and carbon dioxide was removed, thereby obtaining a scanning spectrum. The data processing software is used to perform baseline correction on the acquired infrared spectrum. 5-point smoothing of the second derivative of Savitzky–Golay and normalized preprocessing were carried out. Then, the original and second derivative spectra of the average infrared spectra of each treatment group were processed by correlation mapping software.

2.8. The Analysis of Common Peak Ratio and Variant Peak Ratio of Infrared Fingerprints.

According to the infrared spectrum, the common peak ratio and the variant peak ratio of the infrared fingerprint can be analyzed. The specific method is as follows:

2.8.1. Determination Method of Common Peak Ratio.

For a group of absorption peaks, if the maximum difference of wave number of absorption peaks is significantly smaller than the average difference of wave number of adjacent absorption peaks, it is determined that the group of peaks is a set of common peaks. The definition of the common peak ratio is as follows:

$$P = \frac{N_g}{N_d} \times 100\%,$$

$$N_d = N_g + n_a + n_b,$$

(2)

where P is the common peak rate and N_g is the number of absorption peaks that appear in both infrared spectrum figures being compared, N_d is the number of independent peaks that appear in the two infrared spectrum figures that are compared with each other, n_a is the number of non-common peaks corresponding to the common peak in the fingerprint a, called the variation of a, and n_b is the number of noncommon peaks corresponding to the common peak in the fingerprint b, called the variation of b.

The definition of the variant peak ratio is as follows:

$$P_{va} = \frac{n_a}{N_g} \times 100\%,$$

$$P_{vb} = \frac{n_b}{N_g} \times 100\%,$$

$$N_a = N_g + n_a,$$

$$N_b = N_g + n_b,$$

(3)

where P_{va} is the variant peak ratio of the fingerprint a, P_{vb} is the variant peak ratio of the fingerprint map b, N_a is the peak number of fingerprint a, and N_b is the peak number of fingerprint b.

Based on the calculation formula of the common peak rate and the variation peak rate of the fingerprint, using each sample as a reference, we can calculate the common peak ratio and the variation peak ratio of the infrared fingerprints of other samples. Then, a sequence is formed according to the values of the common peak ratio (including the values of the common peak ratio and the variation peak ratio), which

is called the double-index sequence of the common peak ratio and the variation peak ratio. Through this sequence, the difference between different needle spacing treatment groups can be accurately analyzed.

2.9. Statistical Analysis. One-way analysis of variance and significance analysis were performed using relevant data analysis software. One-way analysis of variance was used to calculate differences in average drying time, average drying rate, polysaccharide content, and flavonoid content of goji berry. Significant differences were expressed as p values ($p < 0.05$ indicates statistically significant differences).

3. Results and Discussion

3.1. Effect of Different Needle Spacings on Average Drying Rate and Average Drying Time of Goji Berry. Figure 2 depicts the average drying rate and average drying time of goji berry under different needle spacings. It can be seen from Figure 2 that the average drying rate of goji berry under different needle spacing conditions is significantly higher than that of the control group. When the moisture content was reduced to 10%, the average drying rate at 2 cm, 4 cm, 6 cm, 8 cm, 10 cm, and 12 cm increased to be 1.6857, 1.5946, 1.5128, 1.4750, 1.4048, and 1.3409 times compared to the control group, respectively. The drying rate of goji berry decreased with the increase of the needle spacing. It was also found that the average drying time of goji berry under different needle spacing conditions is significantly shorter than that of the control group. The drying time of goji berry increased with the increase of the needle spacing. The average total drying rate is inversely proportional to the average total drying time under different needle spacing drying conditions. The longer the drying time is, the lower the drying rate is.

3.2. Effect of Different Needle Spacings on Flavonoid Content and Polysaccharide Content of Goji Berry. Figure 3 depicts the changes in polysaccharide content and flavonoid content of goji berry under different needle spacing conditions. It can be seen from Figure 3 that the electrohydrodynamic drying has no negative influence on the polysaccharide content of goji berry. The polysaccharide content also changed as the needle spacing changed. The polysaccharide content was the highest (16.0 g/100 g) at 4 cm and the least (12.3 g/100 g) at 10 cm and 12 cm. The flavonoid content was highest (0.13 g/100 g) at 2 cm and the lowest (0.08 g/100 g) at 6 cm. It shows that the needle spacing can have a certain influence on the active ingredients inside the goji berry during the drying process. Yang et al. reported that, compared with the hot-air drying, the polysaccharide content of goji berry dried electrohydrodynamically significantly increased [18]. Song et al. found that under freeze-drying process, the flavonoid content of goji berry using distilled water pretreatment was much higher than that of sodium carbonate [26]. These research results showed that different drying methods and conditions have a significant effect on the nutrients of goji berry, which is consistent with our experimental results.

3.3. First-Order Infrared Spectrum Analysis of Dried Goji Berry with Different Needle Spacings. Figure 4 depicts the first-order infrared spectrum of dried goji berry under different needle spacing conditions. It can be seen from Figure 4 that the first-order infrared spectra under the different needle spacing conditions are generally similar. The positions of the peaks and the peak heights are relatively close. However, the intensity of the characteristic peaks is different, and the absorbance decreases with the increase of the needle spacing. Compared with the control group, the peak positions are similar and the characteristic peak intensity is larger. It is indicated that the chemical composition of the different needle spacing treatment groups is basically the same as that of the control group, and the preservation of the chemical composition may be more significant. From Figure 4, we can see that the first-order infrared spectra of dried goji berry with different needle spacings have some typical characteristic peaks. Each compound makes its own contribution to the overall spectrum, depending on the types of bonds it contains and what its overall concentration in the sample is [19]. In the infrared spectrum, each peak represents some components of goji berry [27]. It is a stretching vibration of polysaccharides, glycosides, amino acids, proteins, and sugar alcohols N-H, O-H in the vicinity of 3430 cm^{-1}. There are methylene and methyl C-H stretching vibrations near the 2929 cm^{-1} and 2855 cm^{-1}. It is a stretching vibration peak of C=O of a carboxylic acid or an ester in the vicinity of 1740 cm^{-1}. It is a vibration peak of amino acid and protein amide I bands, III bands, alkaloids, and unsaturated esters in the vicinity of 1630 cm^{-1}, 1360 cm^{-1}, and 1260 cm^{-1}. It belongs to the bending vibration of C-OH of carbohydrates such as glycosides and polysaccharides near 1083 cm^{-1}.

3.4. First-Order Infrared Spectrum Peak Intensity Ratio Analysis of Dried Goji Berry with Different Needle Spacings. Figure 5 depicts the absorption peak intensity ratio of the first-order infrared spectrum of dried goji berries with different needle spacings. It can be seen that the absorption peak intensity ratios of the 3425 cm^{-1}/2925 cm^{-1} were 2.1385, 1.3859, 1.2420, 1.2165, 1.0867, 1.0844, and 1.09582, respectively, at the control, 2 cm, 4 cm, 6 cm, 8 cm, 10 cm, and 12 cm. The absorption peak intensity ratios of the 2925 cm^{-1}/2852 cm^{-1} were 1.0470, 1.0441, 1.0321, 1.2651, 1.0229, 1.0235, and 1.01665, respectively, at the control, 2 cm, 4 cm, 6 cm, 8 cm, 10 cm, and 12 cm. The intensity ratio of the absorption peaks of 3425 cm^{-1}/2925 cm^{-1} and 2925 cm^{-1}/2852 cm^{-1} gradually decreases with the increase of the needle spacing, and the overall trend is downward. The absorption peak intensity ratios of the 3425 cm^{-1}/1601 cm^{-1} were 0.8145, 0.9504, 0.9817, 0.9691, 1.0170, 1.0145, and 1.0807, respectively, at the control, 2 cm, 4 cm, 6 cm, 8 cm, 10 cm, and 12 cm. The absorption peak intensity ratios of the 2925 cm^{-1}/1601 cm^{-1} were 0.3808, 0.6857, 0.8009, 0.7966, 0.9358, 0.9355, and 0.9862, respectively, at the control, 2 cm, 4 cm, 6 cm, 8 cm, 10 cm, and 12 cm. The intensity ratios of the first-order infrared spectra of the different needle spacing treatment groups of 3425 cm^{-1}/1601 cm^{-1} and 2925 cm^{-1}/
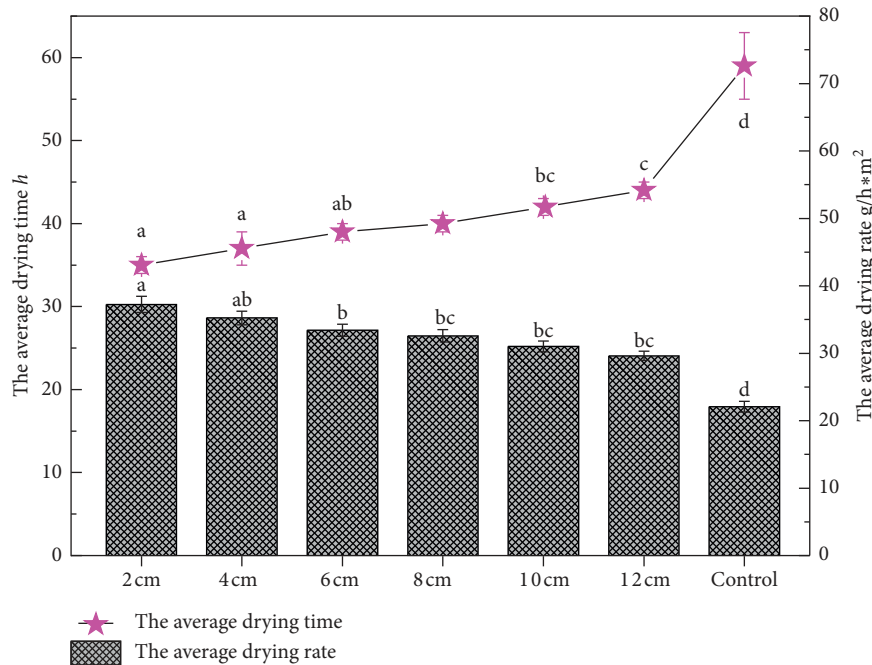
FIGURE 2: Changes in average drying rate and average drying time of goji berry at different needle spacings. Data are shown as the mean ± SD. For each response, means with different lowercase letters are significantly different ($p < 0.05$).
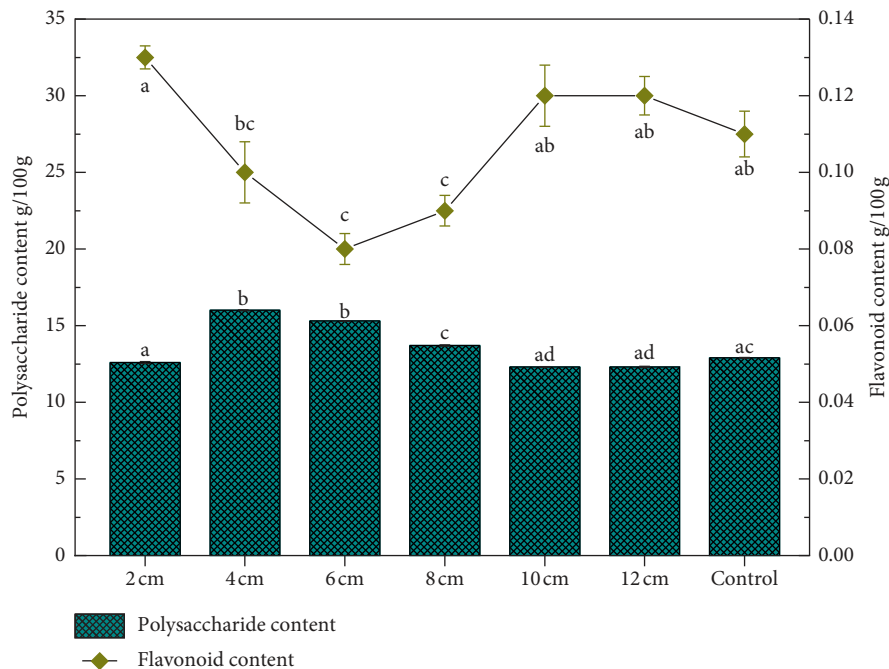

FIGURE 3: Changes in polysaccharide content and flavonoid content of goji berry at different needle spacings. Data are shown as the mean ± SD. For each response, means with different lowercase letters are significantly different ($p < 0.05$).

$1601 \, cm^{-1}$ gradually increased with the increase of the needle spacing, and the overall trend was upward. According to Figure 5, from the peak intensity ratio of infrared spectrum of goji berry, it can be seen that the electrohydrodynamic drying has a significant effect on the internal active components of goji berry, and the effect on different ingredients is different.

3.5. Second-Order Infrared Spectrum Analysis of Dried Goji Berry with Different Needle Spacings. Based on the original infrared spectrum and the intensity ratio of different absorption peaks of the original infrared spectrum, the resolution of the infrared spectrum of different needle spacing is improved by second derivative infrared spectroscopy and differentiated. As can be seen from Figure 6, there was no
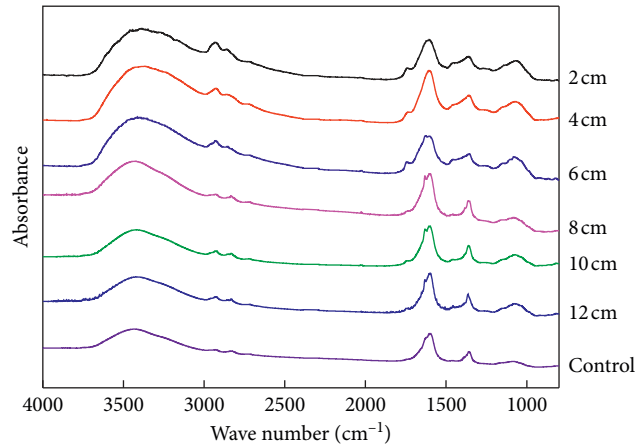
FIGURE 4: First-order infrared spectrum of dried goji berry with different needle spacings.

(a)

(b)

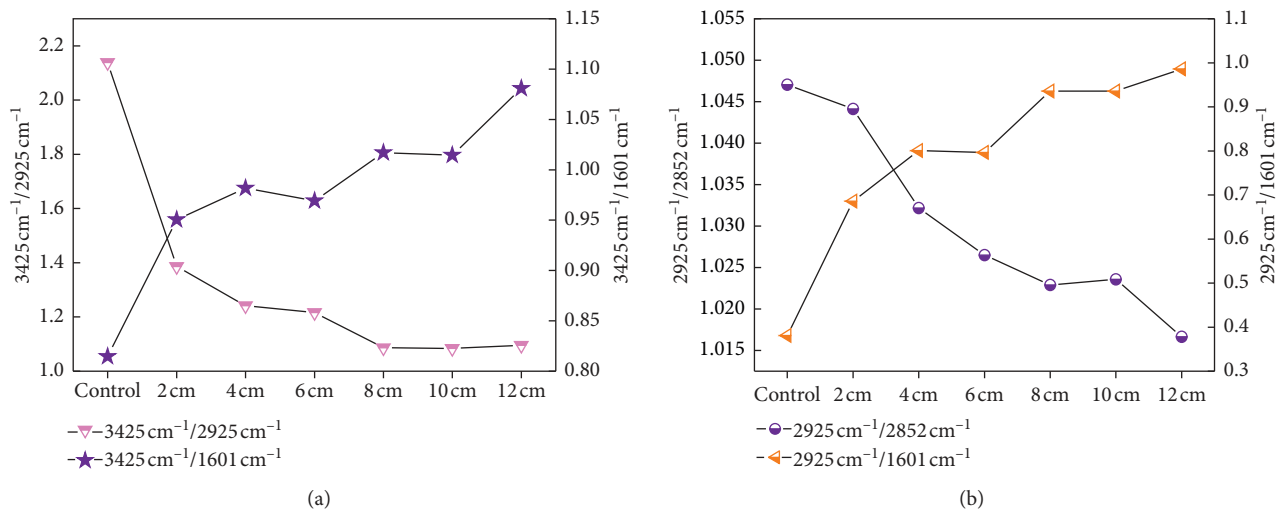FIGURE 5: First-order infrared spectrum peak intensity ratio of dried goji berry with different needle spacings. (a) The absorption peak intensity ratios of $3425\,cm^{-1}/2925\,cm^{-1}$ and $3425\,cm^{-1}/1601\,cm^{-1}$. (b) The absorption peak intensity ratios of $2925\,cm^{-1}/2852\,cm^{-1}$ and $2925\,cm^{-1}/1601\,cm^{-1}$.
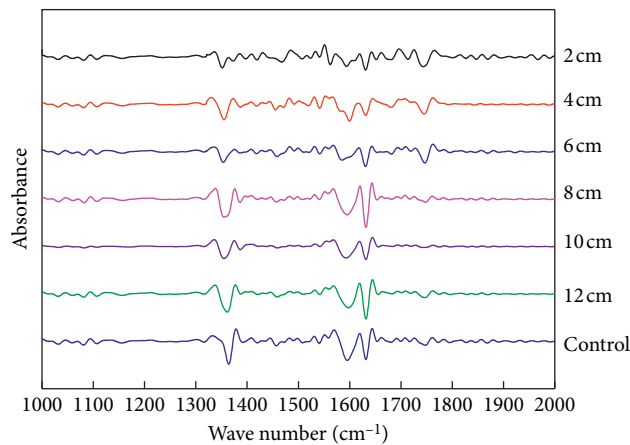

FIGURE 6: Second-order infrared spectrum of dried goji berry with different needle spacings.

obvious absorption peak near 1740 cm^{-1} in the control group, while a strong and wide absorption peak appeared in the 2 cm, 4 cm, and 6 cm treatment groups, and the peak value gradually decreased with the increase of needle spacing. It was also found that the control group had stronger second-order infrared spectral absorption peak near 1350 cm^{-1}, 1601 cm^{-1}, and 1630 cm^{-1} than the electrohydrodynamic treatment group, and the peak value gradually decreased with the increase of needle spacing. Therefore, it was proved that goji berries using electrohydrodynamic drying were significantly different from the control group in terms of protein, polysaccharide, and lipid content. In the second-order derivative infrared spectrum of the electrohydrodynamically dried goji berry, the treatment groups with different needle spacings have their own distinct characteristic peaks, which are easy to be distinguished.

3.6. Double-Index Sequence Analysis of Common Peak Ratio and Variant Peak Ratio of Goji Berry Infrared Fingerprints under Different Needle Spacing Conditions.

Using the double indicators of common peak ratio and variant peak ratio, two fingerprints can be comprehensively described from the commonality and the difference. The higher the common peak ratio, the greater the commonality of the two fingerprints. In the variability peak rate index, the variation of the fingerprint spectrum can be well measured by the ratio of the number of mutated peaks and the number of common peaks in each fingerprint. The larger the variation of the peak rate of the two fingerprints is, the greater the difference in the effect of different needle spacings is. The smaller the variant peak ratio of the two fingerprints is, the closer the properties of the two treatment groups is, and then the smaller the variation is. In this experiment, seven treatment groups were established as reference points to establish a 7-dimensional sequence space with seven common peak ratio and variant peak ratio double-index sequences. Adding the common indicator peak rate and the variant peak ratio double-index space, the similarities and differences between the processing groups can be examined in the 2 + n dimension (n is the number of samples), which makes the method have strong discriminating ability.

Based on the method of determining the common peak, we can find multiple sets of common peaks from Table 1. For the two sets of peaks corresponding to 1740 cm^{-1} and 1625 cm^{-1}, the average wave number of the group corresponding to 1740 cm^{-1} is 1773.43 cm^{-1}. The maximum wave number difference in the group is 12 cm^{-1}. The difference between the wave numbers of the two groups before and after is 984.97 cm^{-1} and 108.43 cm^{-1}, respectively. The two values are significantly larger than 12, so it can be confirmed that a group of peaks corresponding to 1740 cm^{-1} is a common peak. Similarly, the average wave number of a set of peaks corresponding to 1599 cm^{-1} is 1601.71 cm^{-1}, and the average wave number difference between the two adjacent peaks is 27.29 cm^{-1} and 144.71 cm^{-1}, which is significantly larger than the maximum wave number difference of 5 cm^{-1} in the group. Therefore, it can be judged that the group of peaks is also a common peak.

Table 1: Wave numbers and common peaks of absorption peaks of goji berry infrared fingerprints under different needle spacing conditions.

Sample	The wave numbers of peaks in IR fingerprint spectra (cm^{-1})								
G1	3430	2960	2929		2831		1740		1599
G2	3420		2928	2855	2832	2717	1744	1628	1600
G3	3428	2956	2929	2853	2832	2719	1733	1630	1601
G4	3422		2927	2854	2832	2719	1740	1629	1602
G5	3421		2928	2863		2729	1733		1604
G6	3368		2928	2863		2728	1732		1604
G7	3383		2932	2861			1740		1602
G1	1462	1357		1083	910	862		776	
G2	1456	1363	1262	1079	919	863		776	
G3	1457	1360		1081	922	866		776	
G4	1457	1361	1261	1078	918	863	817	776	
G5		1358	1273	1072	914	879		777	
G6		1359	1271	1072			818	775	
G7	1453	1361	1272	1062			815	779	

The results of the double-index sequence analysis of goji berry infrared fingerprints under different needle spacing conditions are shown in Table 2:

Group A: G2 : G3 (87.5%; 7.0, 7.0), G3 : G2 (87.5%; 7.0, 7.0), G2 : G4 (93.8%; 0, 6.7), and G2 : G4 (93.8%; 6.7, 0).

Group B: G1 : G6 (43.8%; 71.4, 57.1), G6 : G1 (43.8%; 57.1, 71.4), G1 : G7 (53.3%; 50.0, 37.5), and G7 : G1 (53.3%; 37.5, 50.0).

In group A, G2 and G3 and G4 have the highest common peak ratio and the smallest variant peak ratio. For different needle spacing treatment groups, the above experimental results show that as the needle spacing increases, the electric field effect decreases, so the variability of the infrared spectrum peak from the 8 cm treatment group to the 12 cm treatment group also becomes smaller and thus has a higher common peak ratio. Therefore, they have the closest relationship and the highest similarity.

In group B, G1 was the control group; G6 and G7 were the 4 cm treatment group and the 2 cm treatment group, respectively. They have a very low common peak ratio and a very high variant peak ratio. From the analysis results of the previous sections, the 2 cm and 4 cm treatment groups have greater differences compared with the control group, which leads to an increase in the variant peak ratio of the infrared spectrum when G1 is compared with G6 and G7.

It can be seen from the above analysis that the common peak rate between the 8 cm, 10 cm, and 12 cm treatment groups is higher. So, the similarity is also higher. It proves that the high-voltage electric field is increased when the needle spacing is increased to 8 cm. The drying effect begins to decrease. It was proved that the electrohydrodynamic drying effect began to decrease when the needle spacing was increased from 8 cm. Compared with the control group, the infrared spectral variability peak rate with high needle spacing density is higher, and the difference is higher. These analyses correctly reflect the actual situation and are similar to our experimental results.

TABLE 2: Double-indicator sequence of goji berry infrared fingerprints under different needle spacing conditions.

Sequence	$(P; P_{va}, P_{vb})$	Sequence	$(P; P_{va}, P_{vb})$	Sequence	$(P; P_{va}, P_{vb})$
G1 : G2	(68.8%; 9.0, 36.4)	G2 : G1	(68.8%; 36.4, 9.0)	G3 : G1	(80.0%; 25.0, 0)
G1 : G3	(80.0%; 0, 25.0)	G2 : G3	(87.5%; 7.0, 7.0)	G3 : G2	(87.5%; 7.0, 7.0)
G1 : G4	(64.7%; 9.0, 45.6)	G2 : G4	(93.8%; 0, 6.7)	G3 : G4	(82.4%; 7.0, 14.3)
G1 : G5	(60.0%; 33.3, 33.3)	G2 : G5	(80.0%; 25.0, 0)	G3 : G5	(68.8%; 36.4, 9.1)
G1 : G6	(43.8%; 71.4, 57.1)	G2 : G6	(62.5%; 50.0, 10.0)	G3 : G6	(52.9%; 66.7, 22.2)
G1 : G7	(53.3%; 50.0, 37.5)	G2 : G7	(62.5%; 50.0, 10.0)	G3 : G7	(52.9%; 66.7, 22.2)
G7 : G1	(53.3%; 37.5, 50.0)	G7 : G2	(62.5%; 10.0, 50.0)	G7 : G3	(52.9%; 22.2, 66.7)
G4 : G1	(64.7%; 45.6, 9.0)	G5 : G1	(60.0%; 33.3, 33.3)	G6 : G1	(43.8%; 57.1, 71.4)
G4 : G2	(93.8%; 6.7, 0)	G5 : G2	(80.0%; 0, 25.0)	G6 : G2	(62.5%; 10.0, 50.0)
G4 : G3	(82.4%; 14.3, 7.0)	G5 : G3	(68.8%; 9.1, 36.4)	G6 : G3	(52.9%; 22.2, 66.7)
G4 : G5	(75.0%; 33.3, 0)	G5 : G4	(75.0%; 0, 33.3)	G6 : G4	(68.8%; 0, 45.5)
G4 : G6	(68.8%; 45.5, 0)	G5 : G6	(77.0%; 20.0, 10.0)	G6 : G5	(77.0%; 10.0, 20.0)
G4 : G7	(68.8%; 45.5, 0)	G5 : G7	(64.3%; 33.3, 22.2)	G6 : G7	(83.3%; 10.0, 10.0)
G7 : G4	(68.8%; 0, 45.5)	G7 : G5	(64.3%; 22.2, 33.3)	G7 : G6	(83.3%; 10.0, 10.0)

Note: G1 : G2 (68.8%; 9.0, 36.4) indicates that the sequence uses G1 as the standard to calculate the common peak ratio and variant peak ratio of the fingerprints of other pretreatment groups. The sequence fragment indicated that the common peak ratio of G1 and G2 was 68.8%, wherein the variation peak rate of G1 was 9.0, and the variation peak rate of G2 was 36.4. G1: control group, G2: 12 cm treatment group, G3: 10 cm treatment group, G4: 8 cm treatment group, G5: 6 cm treatment group, G6: 4 cm treatment group, and G7: 2 cm treatment group.

4. Conclusions

The average drying rate of goji under different needle spacing conditions was significantly higher than that of the control group. The average drying rate decreased with the increase of needle spacing. Changes in needle spacing can cause changes in the quality parameters of goji berry such as polysaccharide content and flavonoid content. The main absorption peak intensity ratio of the first-order infrared spectrum of goji berry in different needle spacing treatment groups showed a certain regularity with the increase of the needle spacing. There are differences in the shape and intensity of the absorption peaks of the second derivative infrared spectrum of goji berry in different needle spacing treatment groups. The double-index sequence analysis of the common peak rate and the variation peak rate of the infrared fingerprint showed that the effect of the electrohydrodynamic drying on the infrared spectrum of the goji berry did not increase significantly after the needle spacing was increased to a certain extent (8 cm). And it was found that the electrohydrodynamic drying had the best effect on goji berry when the needle spacing was 2 cm and 4 cm.

Data Availability

The data used to support the findings of this study are included within the article.

Conflicts of Interest

The authors declare that there are no conflicts of interest regarding the publication of this paper.

Acknowledgments

References

[1] M. Arslan, X. Zou, H. E. Tahir et al., "Near-infrared spectroscopy coupled chemometric algorithms for prediction of antioxidant activity of black goji berries (*Lycium ruthenicum* Murr.)," *Journal of Food Measurement and Characterization*, vol. 12, no. 6, pp. 2366–2376, 2018.

[2] Q. Li, X. Yu, and J.-M. Gao, "A novel method to determine total sugar of goji berry using FT-NIR spectroscopy with effective wavelength selection," *International Journal of Food Properties*, vol. 20, no. 1, pp. S478–S488, 2017.

[3] H. Amagase and N. R. Farnsworth, "A review of botanical characteristics, phytochemistry, clinical relevance in efficacy and safety of *Lycium barbarum* fruit (Goji)," *Food Research International*, vol. 44, no. 7, pp. 1702–1717, 2011.

[4] L. Gan, S. Hua Zhang, X. Bi Xu, and H. B. Xu, "Immunomodulation and antitumor activity by a polysaccharide-protein complex from Lycium barbarum," *International Immunopharmacology*, vol. 4, no. 4, pp. 563–569, 2004.

[5] J. Zheng, C. Ding, L. Wang et al., "Anthocyanins composition and antioxidant activity of wild *Lycium ruthenicum Murr.* from Qinghai-Tibet Plateau," *Food Chemistry*, vol. 126, no. 3, pp. 859–865, 2011.

[6] D. Zhao, J. Wei, J. Hao et al., "Effect of sodium carbonate solution pretreatment on drying kinetics, antioxidant capacity changes, and final quality of wolfberry (*Lycium barbarum*) during drying," *LWT*, vol. 99, pp. 254–261, 2019.

[7] L. Xie, A. S. Mujumdar, X.-M. Fang et al., "Far-infrared radiation heating assisted pulsed vacuum drying (FIR-PVD) of wolfberry (Lycium barbarum L.): effects on drying kinetics and quality attributes," *Food and Bioproducts Processing*, vol. 102, pp. 320–331, 2017.

[8] G. Liu, J. Wang, F. Zhu et al., "Effects of different drying methods on the quality of micronized Chinese wolfberry powder," *Medicinal Plant*, vol. 8, no. 4, 2017.

[9] A. Martynenko, T. Astatkie, and T. Defraeye, "The role of convection in electrohydrodynamic drying," *Journal of Food Engineering*, vol. 271, Article ID 109777, 2019.

[10] T. Defraeye and A. Martynenko, "Future perspectives for electrohydrodynamic drying of biomaterials," *Drying Technology*, vol. 36, no. 1, pp. 1–10, 2018.

[11] C. A. Shi, A. Martynenko, T. Kudra, P. Wells, K. Adamiak, and G. S. P. Castle, "Electrically-induced mass transport in a multiple pin-plate electrohydrodynamic (EHD) dryer," *Journal of Food Engineering*, vol. 211, pp. 39–49, 2017.

[12] T. Kudra and A. Martynenko, "Electrohydrodynamic drying: theory and experimental validation," *Drying Technology*, vol. 38, p. 168, 2020.

[13] H. Yu, A. Bai, X. Yang, and Y. Wang, "Electrohydrodynamic drying of potato and process optimization," *Journal of Food Processing and Preservation*, vol. 42, no. 2, Article ID e13492, 2018.

[14] C. Ding, J. Lu, and Z. Song, "Electrohydrodynamic drying of carrot slices," *Plos One*, vol. 10, no. 4, Article ID e0124077, 2015.

[15] A. Esehaghbeygi, K. Pirnazari, and M. Sadeghi, "Quality assessment of electrodynamic and microwave dehydrated banana slices," *LWT-Food Science and Technology*, vol. 55, no. 2, pp. 565–571, 2014.

[16] Y. Bai, Y. Yang, and Q. Huang, "Combined electrohydrodynamic (EHD) and vacuum freeze drying of sea cucumber," *Drying Technology*, vol. 30, no. 10, pp. 1051–1055, 2012.

[17] M. Yang and C. Ding, "Electrohydrodynamic (EHD) drying of the Chinese wolfberry fruits," *Springerplus*, vol. 5, no. 1, p. 909, 2016.

[18] M. Yang, C. Ding, and J. Zhu, "The drying quality and energy consumption of Chinese wolfberry fruits under electrohydrodynamic system," *International Journal of Applied Electromagnetics and Mechanics*, vol. 55, no. 1, pp. 101–112, 2017.

[19] S. Bureau, D. Cozzolino, and C. J. Clark, "Contributions of Fourier-transform mid infrared (FT-MIR) spectroscopy to the study of fruit and vegetables: a review," *Postharvest Biology and Technology*, vol. 148, pp. 1–14, 2019.

[20] H. Zhuang, Y. Ni, and S. Kokot, "A comparison of near- and mid-infrared spectroscopic methods for the analysis of several nutritionally important chemical substances in the Chinese yam (Dioscorea opposita): total sugar, polysaccharides, and flavonoids," *Applied Spectroscopy*, vol. 69, no. 4, pp. 488–495, 2015.

[21] G. Acri, B. Testagrossa, and G. Vermiglio, "FT-NIR analysis of different garlic cultivars," *Journal of Food Measurement and Characterization*, vol. 10, no. 1, pp. 127–136, 2016.

[22] S. Tingting, Z. Xiaobo, S. Jiyong et al., "Determination geographical origin and flavonoids content of goji berry using near-infrared spectroscopy and chemometrics," *Food Analytical Methods*, vol. 9, no. 1, pp. 68–79, 2016.

[23] M. Arslan, Z. Xiaobo, H. Xuetao et al., "Near infrared spectroscopy coupled with chemometric algorithms for predicting chemical components in black goji berries (*Lycium ruthenicum Murr.*)," *Journal of Near Infrared Spectroscopy*, vol. 26, no. 5, pp. 275–286, 2018.

[24] Z. H. Tekin and M. Baslar, "The effect of ultrasound-assisted vacuum drying on the drying rate and quality of red peppers," *Journal of Thermal Analysis and Calorimetry*, vol. 132, no. 2, pp. 1131–1143, 2018.

[25] L. Xie, Z.-A. Zheng, A. S. Mujumdar et al., "Pulsed vacuum drying (PVD) of wolfberry: drying kinetics and quality attributes," *Drying Technology*, vol. 36, no. 12, pp. 1501–1514, 2018.

[26] H. Song, J. Bi, Q. Chen, M. Zhou, X. Wu, and J. Song, "Structural and health functionality of dried goji berries as affected by coupled dewaxing pre-treatment and hybrid drying methods," *International Journal of Food Properties*, vol. 21, no. 1, pp. 2527–2538, 2018.

[27] J. Ni, C. Ding, Y. Zhang, Z. Song, X. Hu, and T. Hao, "Electrohydrodynamic drying of Chinese wolfberry in a multiple needle-to-plate electrode system," *Foods*, vol. 8, no. 5, p. 152, 2019.